Synthesis and Optical Property of a New Zinc Complex Based on the Derivative of 2-(2′-Hydroxyphenyl)-1H-benzimidazole and Phenanthroline①

YIN Guo-Jie[a②] ZHANG Hao-Yu[a] TIAN Wen-Jie[a]
ZHAO Dan[a] ZHANG Bin[b②] CHEN Dong-Mei[a]

[a] (*School of Environmental Engineering and Chemistry, Luoyang Institute of Science and Technology, Luoyang* 471023, *China*)

[b] (*College of Chemistry, Zhengzhou University, Zhengzhou* 450000, *China*)

ABSTRACT A novel zinc complex (ZnE) has been designed and synthesized based on the derivative of 2-(2′-hydroxyphenyl)-1-H-benzimidazole (HBI) and the neutral nitrogen-containing ligand (phen). The crystal of the title complex crystallizes in the monoclinic system, space group $P2_1/n$ with a = 10.2631(2), b = 34.2166(6), c = 11.4103(3) Å, β = 96.771(2)°, M_r = 844.24, V = 3978.99(14) Å^3, Z = 4, the final R = 0.0400 and wR = 0.1001 for 8107 observed reflections ($I > 2\sigma(I)$). In the title complex, the free protonated phenoxide moiety (4-OH) is successfully retained to realize pseudo-intramolecular hydrogen bonds with the coordinated O atom from the other ligand.

Keywords: synthesis, proton transfer, intramolecular hydrogen bond;

DOI: 10.14102/j.cnki.0254–5861.2011–2941

1 INTRODUCTION

Recently, fluorophore based on excited-state intramolecular proton transfer (ESIPT) in particular has attracted considerable attention from both experimental and theoretical viewpoints, because it show uniquely optical properties[1-5]. A dual emission originating from both the initial excited form and the proton-transferred tautomer is usually found by the ESIPT chromophores, which are of special interest in white light-emitting materials[6-8], and a large panel of optical applications based on ESIPT lumophores has been made[9-13]. Despite these encouraging results, syntheses of hydroxybenzazole derivatives for efficient ESIPT emission with different color are challenged until now[14-19]. It is well established that ESIPT is a fast photoisomerization process, which mainly relies on the keto-enol tautomerism. Upon photoexcitation, the enol conformer (–O–H ···N= or –N–H ···N=) of these compounds undergoes ultrafast intramolecular proton transfer to afford the excited keto tautomer (=O ···H–N– or =N ···H–N=)[20-26].

It is well known that the metal ion in the complexes provide the best combination of versatility, stability and efficiency, which provide opportunities for harnessing satisfactory photo-properties[27]. Thus, achieving ESIPT fluorophore based on the pseudo-intramolecular hydrogen bond in complexes is one of our recent targets of fundamental research. The zinc complexes based on 2-(2′-hydroxyphenyl) benzimidazole (HBI) are excellent emitting materials with desired physical and optical properties[28]. Meanwhile, hydroxybenzazole derivatives are the most extensively studied ESIPT fluorophores due to its relative good performance in photoluminescence[29, 30]. In this report, the HBI was functionalized with additional hydroxy moiety in the 4 position and methoxy moiety in the 4′ position to form the 2-(2′-hydroxy-4′-methoxyphenyl)-1-ethyl-4-hydroxybenzimidazole (EtL). Moreover, in order to achieve better proton transfer luminescence, a neutral nitrogen-containing ligand was introduced on the basis of the original complex structure[31]. Upon complexation with Zn(II) ions and the ligands, as expected, the free protonated phenoxide moiety

Received 20 July 2020; accepted 13 October 2020 (**CCDC 2017298**)

① The project was supported by the Training Plan for Young Key Teachers in Colleges and Universities of Henan Province (No. 2020GGJS243) and Scientific and Technological Project of Henan Province (Nos. 182102210102 and 202102210058)

② Corresponding authors. E-mail: 591941522@qq.com and 13523612522@163.com

(4-OH) is successfully retained to realize pseudo-intramolecular hydrogen bonds with the coordinated O atom from the other ligand (Scheme 1). It is looking forward to obtain excited state proton transfer luminescent material with better luminescence property.

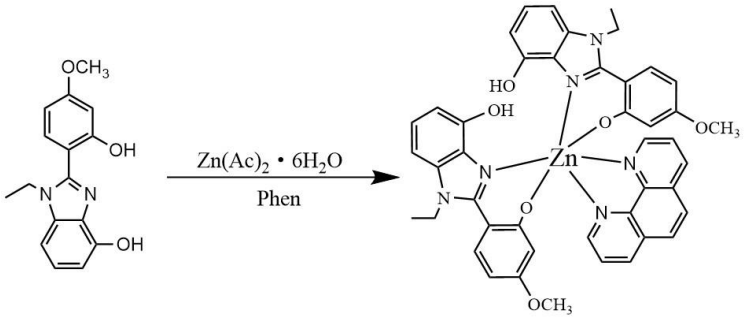

Scheme 1. Structure of the zinc complex ZnE

2 EXPERIMENTAL

All the purchased solvents, except for C_2H_5OH and CH_3OH, were distilled from appropriate drying agents prior to use. The commercially available reagents were used as received, unless otherwise stated. 1H NMR spectra of the compounds were recorded on a Bruker DPX-400MHz spectrometer in DMSO-d_6. Electrospray ionization (ESI) mass spectra of the compounds were conducted in positive ion mode using a Bruker Esquire 3000 instrument in CH_3OH. Elemental analysis for C, H, and N were acquired by employing Carlo-Erba1106 Elemental Analyzer. The absorption spectra were recorded by using Perkin-Elmer Lambda 900 spectrometer. Steady state excitation and emission spectra of the compounds were carried out on a Jobin-Yvon-Horiba FluoroMax-4P spectrometer.

According to the classic benzimidazoles synthesis[32, 33], the ligand 2-(2′-hydroxy-4′-methoxyphenyl)-1-ethyl-4-hydroxylbenzimidazole (EtL) was synthesized in good yield by the reaction with 2-amino-3-nitrophenol and the corresponding salicylaldehyde (Scheme 2). Subsequent reaction of the ligand (EtL) with zinc(II) acetate in methanol afforded zinc complexes (ZnE). Note that easy and specific synthesis of the complex is essential for real applications.

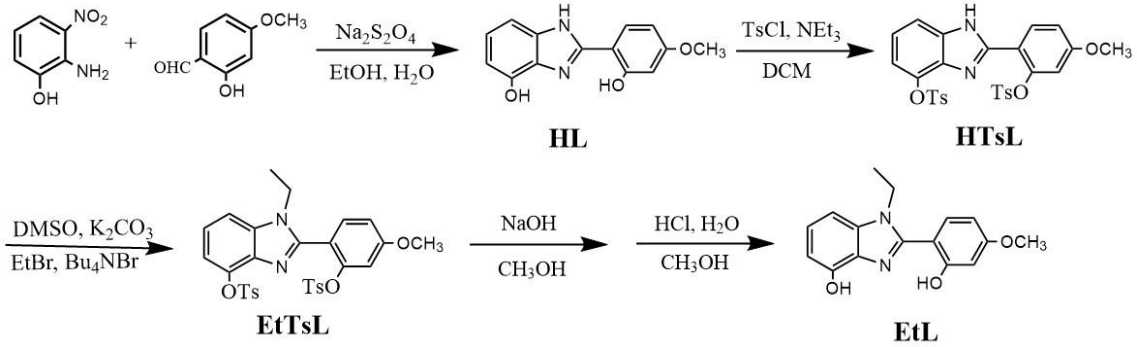

Scheme 2. Synthesis of the ligand EtL

2. 1 Preparation of HL

2-Amino-3-nitrophenol (15 mmol, 2.31 g) and 2-hydroxy-4-methory-benzaldehyde (17 mmol, 3.06 g) were dissolved in 300 mL of a 5:1 EtOH/H_2O mixture. Then $Na_2S_2O_4$ (45 mmol, 7.83 g) was added to it. After heating at 70 ℃ for 5 h, the reaction mixture was cooled to room-temperature and poured into water under stirring. The precipitate was filtered and purified by column chromatography on silica gel using a mixture of ethyl acetate and *n*-hexane as eluent to afford a white powder. Yield: 87.5% (3.36 g). 1H NMR (400 MHz, DMSO): δ 13.44 (s, 1H), 12.92 (d, J = 31.8 Hz, 1H), 10.02 (d, J = 92.1 Hz, 1H), 8.20～7.91 (m, 1H), 7.14～6.98 (m, 2H), 6.70～6.60 (m, 3H), 3.81 (s, 3H); ESI-MS (m/z): 256.9 $[M+l]^+$. Elemental analysis calcd. (%) for $C_{14}H_{12}N_2O_3$: C, 65.62; H, 4.72; N, 10.93. Found (%): C, 65.65; H, 4.69; N, 10.92.

2. 2 Preparation of HTsL

HL (7 mmol, 1.79 g) and triethylamine (3.5 mL, 25 mmol)

were dissolved in CH_2Cl_2 (20 mL). The mixture was cooled to 0 ℃, and then 4-methylbenzenesulfonyl chloride (1.37 g, 7.2 mmol) in CH_2Cl_2 (10 mL) was added dropwise under N_2. After worming the reaction mixture to room temperature for 2 h, it was quenched by water. The mixture was extracted by dichloromethane. The organic layer was dried with Na_2SO_4 and concentrated under reduced pressure. The crude residue was purified by silica gel column chromatography with ethyl acetate/*n*-hexane as eluent to afford a white powder. Yield: 85% (3.36 g) yield. ^{1}H NMR (400 MHz, DMSO) δ 12.42 (s, 1H), 7.86 (d, J = 8.3 Hz, 2H), 7.60 (d, J = 8.7 Hz, 1H), 7.47～7.28 (m, 5H), 7.20～7.08 (m, 2H), 6.95～6.80 (m, 4H), 3.85 (s, 3H), 2.36 (s, 3H), 2.12 (s, 3H); ESI-MS (m/z): 565.3 $[M+l]^+$. Anal. Calcd. (%) for $C_{28}H_{24}N_2O_7S_2$: C, 59.56; H, 4.28; N, 4.96. Found (%): C, 59.59; H, 4.29; N, 4.96.

2. 3 Preparation of EtL

Under N_2 atmosphere, a mixture of HTsL (2 mmol, 1.13 g) and tetrabutylammonium bromide (TBAB, 64.5 mg, 0.2 mmol) were dissolved in DMSO (10 mL). Aqueous K_2CO_3 (2 M, 3.3 mL) was added dropwise to the solution and stirred at room temperature for 1 h. Then ethyl bromide (0.16 mL, 2.2 mmol) was added slowly. The reaction mixture was refluxed for 12 h. After cooling to room temperature, the mixture was poured into water and extracted by dichloromethane. The organic phase was then dried (Na_2SO_4), evaporated, and concentrated to dryness under reduced pressure. The resulting crude product (EtTsL) was dissolved in methanol (20 mL) and refluxed for 2 h after the addition of aqueous NaOH (2.0 mol/L, 5 mL). The mixture was cooled and neutralized by dilute aqueous HCl. The mixture was then extracted by ethyl acetate and the organic layers were dried with Na_2SO_4. The solvent was removed under reduced pressure, and the crude product was further purified by silica gel column chromatography using ethyl acetate/*n*-hexane as eluent to afford a white powder. Yield: 74% (0.42 g). ^{1}H NMR (400 MHz, DMSO) δ 12.11 (s, 1H), 9.92 (s, 1H), 7.55 (d, J = 8.5 Hz, 1H), 7.11～6.97 (m, 2H), 6.69～6.56 (m, 3H), 4.29 (q, J = 7.1 Hz, 2H), 3.80 (s, 3H), 1.34 (t, J = 7.2 Hz, 3H); ESI-MS (m/z): 285.2 $[M+l]^+$. Anal. Calcd. (%) for $C_{16}H_{16}N_2O_3$: C, 67.59; H, 5.67; N, 9.85. Found (%): C, 67.57; H, 5.66; N, 9.86.

2. 4 Synthesis of ZnE

$Zn(Ac)_2$ $2H_2O$ (0.22 g, 1 mmol) in methanol (5 mL) was added in drops to a solution of EtL (2 mmol, 0.57 g) in methanol (30 mL) and 1,10-phenanthroline (Phen) (0.18 g, 1 mmol). The resulting mixture was stirred and refluxed for 5 h. The precipitate was then filtered and recrystallized in methanol as white powder. Colorless single crystals suitable for X-ray diffraction analysis were obtained by slow evaporation of their methanol solutions in air. Yield: 61% (0.51 g). ESI-MS (m/z): 811.4 $[M+l]^+$. Anal. Calcd. (%): C, 65.07; H, 4.72; N, 10.35. Found (%): C, 65.02; H, 4.73; N, 10.33.

2. 3 X-ray crystallography studies of ZnE

Crystal diffraction data for complexes ZnE were collected on an Oxford Diffraction Xcalibur CCD diffractometer using graphite-monochromatized Mo$K\alpha$ radiation (λ = 0.7107 Å) at 293 K by an ω-scan technique. Program CrysAlisPro was employed for data collection and reduction[34]. The structure was solved by direct methods, and refined anisotropically by full-matrix least-squares method on F^2 using the OLEX2-1.2 and SHELX[35, 36]. All non-hydrogen atoms were refined anisotropically. The hydrogen atoms were included in the structure factor calculation at idealized positions using a riding model and refined isotropically. Hydroxyl protons were located from the difference-Fourier map and refined isotropically, and no restrictions were put on the O–H distances. The coordinated water molecule of ZnE was refined to be disordered over two possible sites with site occupancy factors of 0.50:0.50. Details of selected bond lengths (Å) and bond angles (°) for the crystals of the title compound are shown in Tables 1 and 2.

Table 1. Selected Bond Lengths (Å) and Bond Angles (°)

Bond	Dist.	Bond	Dist.	Bond	Dist.
Zn(1)–O(1)	2.0533(15)	Zn(1)–N(1)	2.1680(18)	Zn(1)–N(5)	2.2294(18)
Zn(1)–O(4)	2.0582(14)	Zn(1)–N(3)	2.2003(17)	Zn(1)–N(6)	2.2609(17)
Angle	(°)	Angle	(°)	Angle	(°)
O(1)–Zn(1)–O(4)	178.29(6)	N(1)–Zn(1)–N(3)	91.97(7)	O(1)–Zn(1)–N(6)	96.41(6)
O(1)–Zn(1)–N(1)	87.54(7)	O(1)–Zn(1)–N(5)	93.12(6)	O(4)–Zn(1)–N(6)	84.40(6)
O(4)–Zn(1)–N(1)	93.88(6)	O(4)–Zn(1)–N(5)	85.65(6)	N(1)–Zn(1)–N(6)	95.01(7)
O(1)–Zn(1)–N(3)	93.54(6)	N(1)–Zn(1)–N(5)	169.58(7)	N(3)–Zn(1)–N(6)	168.07(7)
O(4)–Zn(1) –N(3)	85.48(6)	N(3)–Zn(1)–N(5)	98.36(7)	N(5)–Zn(1)–N(6)	74.58(6)

Table 2. Hydrogen Bond Lengths (Å) and Bond Angles (°)

D–H ··A	d(D–H)	d(H ··A)	d(D ··A)	∠DHA
O(2)–H ··O(4)	0.82	1.76	2.557(4)	165
O(5)–H ··O(1)	0.82	1.85	2.656(4)	166

3 RESULTS AND DISCUSSION

In order to elucidate the structure features of the zinc complex (ZnE), the crystal was grown by evaporation of their methanol solutions in air. The complex crystallizes in monoclinic with space group $P1_{21}/n_1$. As shown in Fig. 1, the zinc ion is six-coordinated by N(1)^O(1) and N(3)^O(4) atoms in the two deprotonated ligands with a bidentate bonding mode and N(5)^N(6) atoms of the phen, forming a deformed octahedral coordination environment. Interestingly, the N(1) and N(3) atoms in the two ligands (EtL) in *cis* together with the N(5)^N(6) of the phen ligand constitute the octahedral equatorial plane. The bond lengths of Zn(1)–N(1) and Zn(1)–N(3) between the znic ion and the nitrogen atoms of the two deprotonated ligands are 2.1680(18) and 2.2003(17) Å, respectively. The bond lengths of Zn(1)–N(5) and Zn(1)–N(6) between the zinc ion and the nitrogen atoms of phen are 2.2294(18) and 2.2609(17) Å, respectively. The two oxygen atoms O(1) and O(4) in the ligand EtL are in trans and occupy two vertices of the octahedron, with the bond lengths of Zn(1)–O(1) and Zn(1)–O(4) being 2.0533(15) and 2.0582(14) Å, respectively. At the same time, the distortion of the two EtL ligands caused by the steric hindrance effect is also slightly different. The dihedral angle of the 2-phenyl group containing O(4) atom and the benzimidazole ring is 48.7°, while the other one containing O(1) atom is 44.2°, so the conjugation degree of benzimidazole itself is further reduced. Furthermore, there are strong intramolecular hydrogen bonds in this complex: O(2)–H(2) ··O(4) (O/O 2.557(4) Å, H ··O 1.76 Å, ∠NHO, 165°) and O(5)–H(5) ··O(1) (O/O 2.656(4) Å, H ··O 1.85 Å, ∠OHO, 166°).

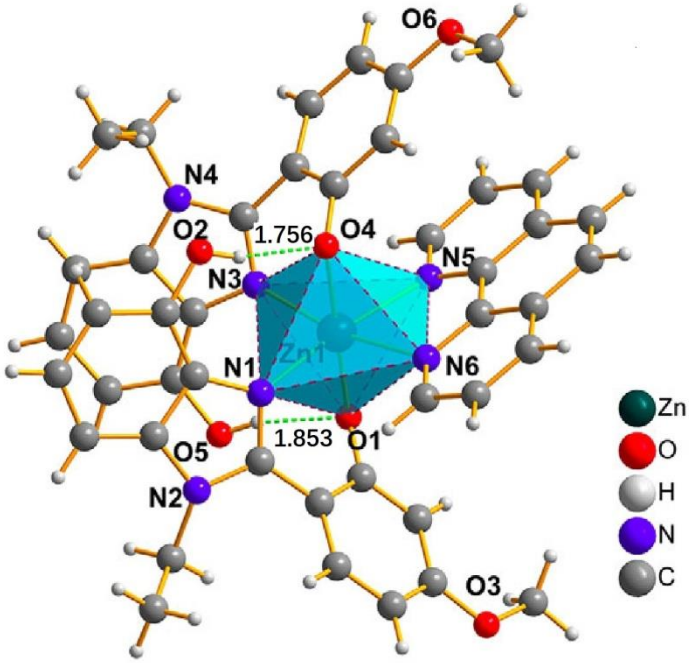

Fig. 1. Molecular structure of the complex ZnE

The UV-Vis absorption spectra of the free ligands (EtL and phen) and the corresponding zinc complex (ZnE) were recorded in methanol solvent at room temperature. As shown in Fig. 2, the main absorption region for the ligand EtL is at 210～220 nm (Table 3), the high-energy absorption bands mainly correspond to the π-π* transition on the 4-hydroxy-benzimidazole moiety, and the lowest-energy absorption bands at ca. 316 nm can be attributed to the coupling between the benzimidazole and the substituted phenyl ring[37, 38]. Upon complexation with Zn(II) ion, the absorption profile is still

dominated by the ligands. Meanwhile, the main absorption wavelength of the ligand phen is in the short-wave region, which enhances the absorption intensity of the complex in the short-wave region. Consequently, due to the dihedral angles between the phenolate and benzimidazole moieties in the complex, the intensity of the long wavelength absorption maxima is reduced relative to that of the maximum absorption wavelengths. It should be noted that the absorption intensities of the complex in the long wavelength region decrease significantly more slowly than that of the corresponding free ligands. The absorption with small extinction coefficient values can be reasonable due to the intramolecular charge-transfer (ICT) between the two coordinated ligands (EtL), as evidenced by the structure, red-shifted absorption tail in addition to the main absorption peak.

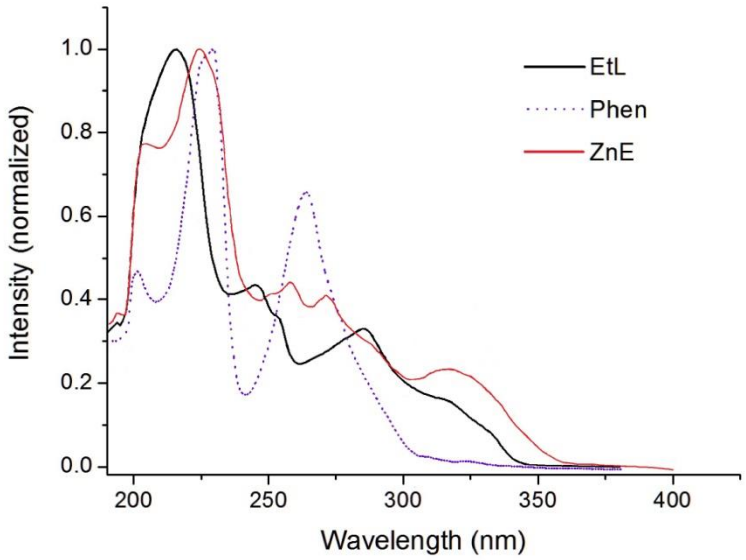

Fig. 2. UV/Vis absorption spectra of the ligand and the zinc complex in methanol solution (1.0×10^{-5} mol·L^{-1})

Table 3. UV/Vis Absorption Data of the Ligand and the Corresponded Zinc Complex in Methanol Solution (1.0×10^{-5} mol·L^{-1})

Compounds	λ_{abs} (nm)
EtL	215, 246, 285, 316
Phen	201, 229, 264
ZnE	204, 225, 258,272, 317

Generally speaking, the HOMO (H) is mainly distributed on electron-rich groups, while LUMO (L) on the electron-deficient group. For the energy of HOMO, the size of the conjugated substituent group has a significant effect. With the increase in delocalized electrons, the energy of HOMO shows an increasing tendency[39]. Furthermore, the HOMO-LUMO gap is an important parameter to characterize the electronic structure of molecule. It is well known that the energy gap retains close connection to some molecular properties[40]. In order to obtain the electronic density distribution of complex, the energy type of the initial spatial configuration was investigated at the B3LYP[41]/3-21G level with density functional theory[42] based on the ground state by using the Gaussian 09 program package[43]. As shown in Fig. 3, the HOMO energy level of –4.78 ev is distributed on the group of ligand EtL and the contribution rate of this moiety in the highest occupied orbital reached 97.6%, while the LUMO energy level of –2.02 ev is distributed on the group of ligand phen and the contribution rate of this moiety in the lowest-unoccupied orbital is up to 98.7% with its energy gap to be 2.68 eV. Therefore, the H→L transition is a predominantly ligand-to-ligand charge transfer transition (LLCT). Normally, the intensity of LLCT is too weak, and it is difficult to observe in the UV/Vis absorption spectrum, which eventually leads to fluorescence quenching.

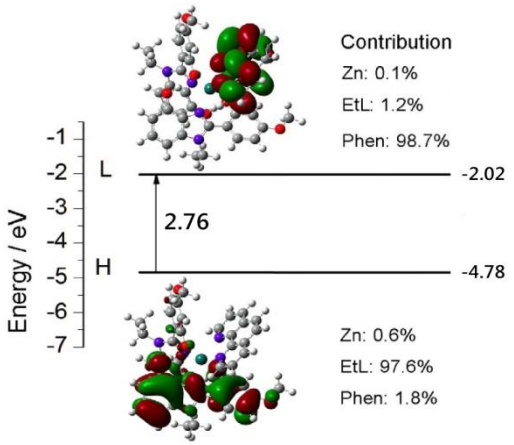

Fig. 3. HOMO-LUMO (H-L) energy levels and the energy gap of the complex

In order to reveal the stability of the crystal structure, thermal gravimetric analysis (TGA) was performed for the complex under nitrogen atmosphere in the range of room temperature to 700 ℃. As depicted in Fig. 4, the initial weight loss of 4.02% from room temperature to 67.6 ℃ corresponded to the release of CH_3OH guest molecules (calcd. 3.79%). After that, there is a plateau region up to 248.2 ℃, and then the weight loss is attributable to the decomposition of the coordination framework. The final residue of 9.81% for compound **2** is in agreement with the percentage of ZnO in all cases (calcd. 9.59%).

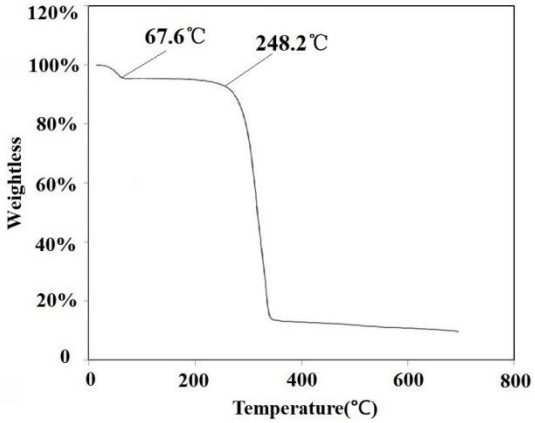

Fig. 4. TGA curve of the complex

4 CONCLUSION

In conclusion, a novel zinc complex has been designed and synthesized based on 2-(2′-hydroxy-4′-methoxy-phenyl)-1-ethyl-4-hydroxybenzimidazole (EtL) and neutral nitrogen-containing ligand (phen). As expected, the free protonated phenoxide moiety (4-OH) is successfully retained to realize pseudo-intramolecular hydrogen bonds with the coordinated O atom from the other ligand. However, unfortunately, the H → L transition in the complex is a predominantly ligand-to-ligand charge transfer transition (LLCT) from the group of hydroxybenzimidazole to the nitrogen-containing ligand, which leads to the fluorescence quenching of the complex. Moreover, the introduction of neutral ligands increased the distance of intermolecular hydrogen bonds within the ligands. The luminescence phenomenon of the complex was not observed under solid conditions at the same time. Next, we will revise the strategy and synthesize a new complex on the basis of the zinc salt and the unique ligand (EtL) to eliminate the phenomenon of fluorescence quenching and the influence of introducing nitrogen-containing neutral ligands on the formation of intramolecular hydrogen bonds so as to achieve better luminescence properties.

REFERENCES

(1) Park, S.; Seo, J.; Kim, S. H.; Park, S. Y. Tetraphenylimidazole-based excited-state intramolecular proton-transfer molecules for highly efficient blue electroluminescence. *Adv. Funct. Mater.* **2008**, 18, 726−731.

(2) Park, S.; Kwon, J. E.; Kim, S. H.; Seo, J.; Chung, K.; Park, S. Y.; Jang, D. J.; Medina B. M.; Gierschner J.; Park, S. Y. A white-light-emitting molecule: frustrated energy transfer between constituent emitting centers. *J. Am. Chem. Soc.* **2009**, 131, 14043−14049.

(3) Porel, M.; Ramalingam, V.; Domaradzki, M. E.; Young, V. G.; Ramamurthy, V.; Muthyala, R. S. Chloride sensing via suppression of excited state intramolecular proton transfer in squaramides. *Chem. Commun*. **2013**, 49, 1633−1635.

(4) Hsu, Y. H.; Chen, Y. A.; Tseng, H. W.; Zhang, Z.; Shen, J. Y.; Chuang, W. T.; Lin, T. C.; Lee, C. S.; Hung, W. Y.; Hung, B. C.; Liu, S. H.; Chou, P. T. Locked ortho- and para-core chromophores of green fluorescent protein; dramatic emission enhancement via structural constraint. *J. Am .Chem. Soc.* **2014**, 136, 11805−11812.

(5) Cui, L.; Baek, Y.; Lee, S.; Kwon, N.; Yoon, J. An AIE and ESIPT based kinetically resolved fluorescent probe for biothiols. *J. Mater. Chem. C* **2016**, 4, 2909−2914.

(6) Kim, S.; Seo, J.; Jung, H. K.; Kim, J. J.; Park, S. Y. White Luminescence from polymer thin films containing excited-state intramolecular proton-transfer dyes. *Adv. Mater.* **2005**, 17, 2077−2082.

(7) Ye, J.; Liu, C.; Ou, C.; Cai, M.; Chen, S.; Wei, Q.; Li, W.; Qian, Y.; Xie, L.; Mi, B.; Gao Z.; Huang, W. Universal strategy for cheap and color-stable single-EML WOLEDs utilizing two complementary-color nondoped emitters without energy transfer. *Adv. Optical Mater.* **2014**, 2, 938−944.

(8) Furukawa, S.; Shono, H.; Mutai, T.; Araki, K. Colorless, transparent, dye-doped polymer films exhibiting tunable luminescence color: Controlling the dual-color luminescence of 2-(2′-hydroxyphenyl)imidazo[1,2-a]pyridine derivatives with the surrounding matrix. *ACS Appl. Mater. Inter.* **2014**, 6, 16065−16070.

(9) Park, S.; Kwon, O. H.; Kim, S.; Park, S.; Choi, M. G.; Cha, M.; Park, S. Y.; Jang, D. J. Imidazole-based excited-state intramolecular proton-transfer materials: synthesis and amplified spontaneous emission from a large single crystal. *J. Am. Chem. Soc.* **2005**, 127, 10070−10074.

(10) Park, S.; Kim, S.; Seo, J.; Park, S. Y. Application of excited-state intramolecular proton transfer (ESIPT) principle to functional polymeric materials. *Macromol. Res.* **2008**, 16, 385−395.

(11) Kim, S. H.; Park, S.; Kwon, J. E.; Park, S. Y. Organic light-emitting diodes with a white-emitting molecule: Emission mechanism and device characteristics. *Adv. Funct. Mater.* **2011**, 21, 644−651.

(12) Benelhadj, K.; Muzuzu, W.; Massue, J.; Retailleau, P.; Charaf-Eddin, A.; Laurent, A. D.; Jacquemin, D.; Ulrich, G.; Ziessel, R. White emitters by tuning the excited-state intramolecular proton-transfer fluorescence emission in 2-(2′-hydroxybenzofuran) benzoxazole dyes. *Chem. Eur. J.* **2014**, 20, 12843−12857.

(13) Mutai, T.; Ohkawa, T.; Shono, H.; Araki, K. The development of aryl-substituted 2-phenylimidazo[1,2-a]pyridines (PIP) with various colors of excited-state intramolecular proton transfer (ESIPT) luminescence in the solid state. *J. Mater. Chem. C* **2016**, 4, 3599−3606.

(14) Shono, H.; Ohkawa, T.; Tomoda, H.; Mutai, T.; Araki, K. Fabrication of colorless organic materials exhibiting white luminescence using normal and excited-state intramolecular proton transfer processes. *ACS Appl. Mater. Inter.* **2011**, 3, 654−657.

(15) Ma, J.; Zhao, J.; Yang, P.; Huang, D.; Zhang, C.; Li, Q. New excited state intramolecular proton transfer (ESIPT) dyes based on naphthalimide and observation of long-lived triplet excited states. *Chem. Commun.* **2012**, 48, 9720−9722.

(16) Park, S.; Kwon, J. E.; Park, S. Y. Strategic emission color tuning of highly fluorescent imidazole-based excited-state intramolecular proton transfer molecules. *Phys. Chem. Chem. Phys.* **2012**, 14, 8878−8884.

(17) Skonieczny, K.; Ciuciu, A. I.; Nichols, E. M.; Hugues, V.; Blanchard-Desce, M.; Flamigni, L.; Gryko, D. T. Bright, emission tunable fluorescent dyes based on imidazole and π-expanded imidazole. *J. Mater. Chem.* **2012**, 22, 20649−20664.

(18) Sakai, K.; Kawamura, H.; Kobayashi, N.; Ishikawa, T.; Ikeda, C.; Kikuchi, T.; Akutagawa, T. Highly efficient solid-state red fluorophores using ESIPT: crystal packing and fluorescence properties of alkoxy-substituted dibenzothiazolylphenols. *CrystEngComm.* **2014**, 16, 3180−3185.

(19) Santos, F. S.; Ramasamy, E.; Ramamurthy, V.; Rodembusch, F. S. Confinement effect on the photophysics of ESIPT fluorophores. *J. Mater. Chem. C* **2016**, 4, 2820−2827.

(20) Mosquera, M.; Penedo, J. C.; R ńos Rodr ǵuez, M. C.; Rodr ǵuez-Prieto, F. Photoinduced inter- and intramolecular proton transfer in aqueous and ethanolic solutions of 2-(2′-hydroxyphenyl)benzimidazole: evidence for tautomeric and conformational equilibria in the ground state. *J. Phys. Chem.* **1996**, 100, 5398−5407.

(21) R ńos V ázquez, S.; R ńos Rodr ǵuez, M. C.; Mosquera, M.; Rodr ǵuez-Prieto, F. Rotamerism, tautomerism, and excited-state intramolecular proton transfer in 2-(4′-N,N-diethylamino-2′-hydroxyphenyl)benzimidazoles: novel benzimidazoles undergoing excited-state intramolecular coupled proton and charge transfer. *J. Phys. Chem. A* **2008**, 112, 376−387.

(22) Brenlla, A.; Rodríguez-Prieto, F.; Mosquera, M.; Ríos, M. A.; Ríos Rodríguez, M. C. Solvent-modulated ground-state rotamerism and tautomerism

and excited-state proton-transfer processes ino-hydroxynaphthylbenzimidazoles. *J. Phys. Chem. A* **2009**, 113, 56−67.

(23) Iijima, T.; Momotake, A.; Shinohara, Y.; Sato, T.; Nishimura, Y.; Arai, T. Excited-state intramolecular proton transfer of naphthalene-fused 2-(2′-hydroxyaryl)benzazole family. *J. Phys. Chem. A* **2010**, 114, 1603−1609.

(24) Chipem, F. A. S.; Dash, N.; Krishnamoorthy, G. Role of nitrogen substitution in phenyl ring on excited state intramolecular proton transfer and rotamerism of 2-(2′-hydroxyphenyl)benzimidazole: a theoretical study. *J. Chem. Phys.* **2011**, 10, 104308−9.

(25) Houari, Y.; Charaf-Eddin, A.; Laurent, A. D.; Massue, J.; Ziessel, R.; Ulrich, G.; Jacquemin, D. Modeling optical signatures and excited-state reactivities of substituted hydroxyphenylbenzoxazole (HBO) ESIPT dyes. *Phys. Chem. Chem. Phys.* **2014**, 16, 1319−1321.

(26) Tseng, H. W.; Liu, J. Q.; Chen, Y. A.; Chao, C. M.; Liu, K. M.; Chen, C. L.; Lin, T. C.; Hung, C. H.; Chou, Y. L.; Lin, T. C.; Wang T. L.; Chou, P. T. Harnessing excited-state intramolecular proton-transfer reaction via a series of amino-type hydrogen-bonding molecules. *J. Phys. Chem. Lett.* **2015**, 6, 1477−1486.

(27) Xu, H.; Chen, R.; Sun, Q.; Lai, W.; Su, Q.; Huang, W.; Liu, X. Recent progress in metal-organic complexes for optoelectronic applications. *Chem. Soc. Rev.* **2014**, 43, 3259−3302.

(28) Jiang, M.; Li, J.; Huo, Y.; Xi, Y.; Yan, J.; Zhang, F. Synthesis, thermoanalysis, and thermal kinetic thermogravimetric analysis of transition metal Co(II), Ni(II), Cu(II), and Zn(II) complexes with 2-(2′-hydroxyphenyl)benzimidazole (HL). *J. Chem. Eng. Data* **2011**, 56, 1185−1190.

(29) Yang, X.; Guo, Y.; Strongin, R. M. Conjugate addition/cyclization sequence enables selective and simultaneous fluorescence detection of cysteine and homocysteine. *Angew. Chem. Int. Ed.* **2011**, 50, 10690−10693.

(30) Shaikh, M.; Dutta Choudhury, S.; Mohanty, J.; Bhasikuttan, A. C.; Nau, W. M.; Pal, H. Modulation of excited-state proton transfer of 2-(2′-hydroxyphenyl)benzimidazole in a macrocyclic cucurbit[7]uril host cavity: dual emission behavior and p*Ka* shift. *Chem. Eur. J.* **2009**, 15, 12362−12370.

(31) Zhang, B.; Gu, M.; Liu, C.; Liu, X.; Gao, N.; Gao, Q.; Zhu, Y.; Tang, M.; Du, C.; Song, M. An ESIPT fluorophore based on zinc-induced intramolecular proton transfer between ligands in the complex. *Eur. J. Inorg. Chem.* **2017**, **45**, 5366−5371.

(32) Yang, D.; Fokas, D.; Li, J.; Yu, L.; Baldino, C. M. A versatile method for the synthesis of benzimidazoles from *o*-nitroanilines and aldehydes in one step via a reductive cyclization. *Synthesis* **2005**, 2005, 47−56.

(33) Benelhadj, K.; Massue, J.; Retailleau, P.; Ulrich, G.; Ziessel, R. 2-(2′-hydroxyphenyl)benzimidazole and 9,10-phenanthroimidazole chelates and borate complexes: Solution- and solid-state emitters. *Org. Lett.* **2013**, 15, 2918−2921.

(34) *CrysAlisPro, Version 1.171.36.20, Agilent Technologies UK Ltd.* Oxford, UK **2013**.

(35) Dolomanov, O. V.; Bourhis, L. J.; Gildea, R. J.; Howard, J. A. K.; Puschmann, H. OLEX2: a complete structure solution, refinement and analysis program. *J. Appl. Crystallogr.* **2009**, 42, 339−341.

(36) Sheldrick G. M. A short history of SHELX. *Acta Crystallogr. Sect. A* **2008**, 64, 112−122.

(37) Yao, H.; Funada, T. Mechanically inducible fluorescence colour switching in the formation of organic nanoparticles of an ESIPT molecule. *Chem. Commun.* **2014**, 50, 2748−2750.

(38) Wu, F.; Ma, L.; Zhang, S.; Wang, Z.; Cheng, X. The nonlinear optical properties of HBI in different solvents. *Mater. Lett.* **2014**, 116, 231−234.

(39) Wong, K. T.; Chen, H. F.; Fang, F. C. Novel spiro-configured pet chromophores incorporating 4,5-diazafluorene moiety as an electron acceptor. *Org. Lett.* **2006**, 8, 3501−3504.

(40) Pearson, R. G. Absolute electronegativity and hardness: application to inorganic chemistry. *Inorg. Chem.* **1988**, 27, 734−740.

(41) Lee, C.; Yang, W.; Parr, R. G. Development of the colle-salvetti correlation-energy formula into a functional of the electron density. *Phys. Rev. B* **1988**, 37, 785−789.

(42) Dreizler, R. M.; Gross E. U. K. *Density Functional Theory*. Heidelberg, Germany: Springer-Verlag **1990**.

(43) Frisch, M. J.; Trucks, G. W.; Schlegel, H. B.; Scuseria, G. E.; Robb, M. A.; Cheeseman, J. R.; Scalmani, G.; Barone, V.; Mennucci, B.; Petersson, G. A.; Nakatsuji, H.; Caricato, M.; Li, X.; Hratchian, H. P.; Izmaylov, A. F.; Bloino, J.; Zheng, G.; Sonnenberg, J. L.; Hada, M.;Ehara, M.; Toyota, K.; Fukuda, R.; Hasegawa, J.; Ishida, M.; Nakajima, T.; Honda, Y.; Kitao, O.; Nakai, H.; Vreven, T.; Montgomery, J. A. Jr.; Peralta, J. E.; Ogliaro, F.; Bearpark, M.; Heyd, J. J.; Brothers, E.; Kudin, K. N.; Staroverov, V. N.; Kobayashi, R.; Normand, J.; Raghavachari, K.; Rendell, A.; Burant, J. C.; Iyengar, S. S.; Tomasi, J.; Cossi, M.; Rega, N.; Millam, J. M.; Klene, M.; Knox, J. E.; Cross, J. B.; Bakken, V.; Adamo, C.; Jaramillo, J.; Gomperts, R.; Stratmann, R. E.; Yazyev, O.; Austin, A. J.; Cammi, R.; Pomelli, C.; Ochterski, J. W.; Martin, R. L.; Morokuma, K.; Zakrzewski, V. G.; Voth, G. A.; Salvador, P.; Dannenberg, J. J.; Dapprich, S.; Daniels, A. D.; Farkas, Ö.; Foresman, J. B.; Ortiz, J. V.; Cioslowski, J.; Fox, D. J. *Gaussian 09, Revision A.02.* Gaussian, Inc., Pittsburgh PA **2009**.